
Generalizing MLPs With Dropouts, Batch Normalization, and Skip Connections

Taewoon Kim

Vrije Universiteit Amsterdam
t.kim@vu.nl

Abstract

A multilayer perceptron (MLP) is typically made of multiple fully connected layers with nonlinear activation functions. There have been several approaches to make them better (e.g. faster convergence, better convergence limit, etc.). But the researches lack structured ways to test them. We test different MLP architectures by carrying out the experiments on the age and gender datasets. We empirically show that by whitening inputs before every linear layer and adding skip connections, our proposed MLP architecture can result in better performance. Since the whitening process includes dropouts, it can also be used to approximate Bayesian inference. We have open sourced our code, and released models and docker images at <https://github.com/tae898/age-gender/>.

1 Introduction

1.1 MLP and its training objective

A multilayer perceptron (MLP) is one of the simplest and the oldest artificial neural network architectures. Its origin dates back to 1958 [1]. Its basic building blocks are linear regression and nonlinear activation functions. One can stack them up to create an MLP with L layers (See Equation 1).

$$\hat{\mathbf{y}} = f^{(L)}(\mathbf{W}^{(L)}, \dots, f^{(2)}(\mathbf{W}^{(2)} f^{(1)}(\mathbf{W}^{(1)} \mathbf{x})), \dots) \quad (1)$$

where \mathbf{x} , $\hat{\mathbf{y}}$, $\mathbf{W}^{(l)}$, and $f^{(l)}$ are an input vector, an output vector, the weight matrix, and the nonlinear activation function at the l th layer, respectively. Nonlinearity is necessary since without it, an MLP will collapse into one matrix. The choice of a nonlinear function is a hyperparameter. ReLU [2] is one of the most widely used activation functions.

In a supervised setup, where we have a pair of a data sample $\mathbf{x}^{(i)}$ and a label $\mathbf{y}^{(i)}$, we aim to reduce the loss (distance) between the model output $\hat{\mathbf{y}}^{(i)}$ and the label $\mathbf{y}^{(i)}$. The loss, $L_{\mathbf{W}^{(1)}, \dots, \mathbf{W}^{(L)}}(\hat{\mathbf{y}}^{(i)}, \mathbf{y}^{(i)})$, is parameterized by the weights of all L layers. If we have m pairs of data samples and labels, $\{(\mathbf{x}^{(1)}, \mathbf{y}^{(1)}), \dots, (\mathbf{x}^{(m)}, \mathbf{y}^{(m)})\}$, the objective is to minimize the expectation of the loss (See Equation 2).

$$\mathbb{E}_{\mathbf{x}, \mathbf{y} \sim \hat{p}_{data}} L_{\mathbf{W}^{(1)}, \dots, \mathbf{W}^{(L)}}(\mathbf{x}, \mathbf{y}) = \frac{1}{m} \sum_{i=1}^m L_{\mathbf{W}^{(1)}, \dots, \mathbf{W}^{(L)}}(\mathbf{x}^{(i)}, \mathbf{y}^{(i)}) \quad (2)$$

Since m can be a large number, we typically batch the m data samples into multiple smaller batches and perform stochastic gradient descent to speed up the optimization process and to reduce memory consumption.

Backpropagation [3] is a useful tool to perform gradient descent. This allows us to easily differentiate the loss function with respect to the weights of all L layers, taking advantage of the chain rule.

So far, we talked about the basics of MLPs and how to optimize them in a supervised setup. In the past decade, there have been many works to improve deep neural network architectures and their performances. In the next section, we'll go through some of the works that can be used to generalize MLPs.

2 Related Work

2.1 Dropout

Dropout [4] was introduced to prevent neural networks from overfitting. Every neuron in layer $l - 1$ has probability $1 - p$ of being present. That is, with the probability of p , a neuron is dropped out and the weights that connect to the neurons in layer l will not play a role. p is a hyperparameter whose optimum value can depend on the data, neural network architecture, etc.

Dropout makes the neural network stochastic. During training, this behavior is desired since this effectively trains many neural networks that share most of the weights. Obviously, the weights that are dropped out won't be shared between the sampled neural networks. This stochasticity works as a regularizer which prevents overfitting.

The stochasticity isn't always desired at test time. In order to make it deterministic, the weights are scaled down by multiplying by p . That is, every weight that once was dropped out during training will be used at test time, but its magnitude is scaled down to account for the fact that it used to be not present during training.

In Bayesian statistics, the trained neural network(s) can be seen as a posterior predictive distribution. The authors compare the performance between the Monte-Carlo model averaging and the weight scaling. They empirically show that the difference is minimal.

In some situations, the stochasticity of a neural network is desired, especially if we want to estimate the uncertainty of model predictions. Unlike regular neural networks, where the trained weights are deterministic, Bayesian neural networks learn the distributions of weights, which can capture uncertainty [5]. At test time, the posterior predictive distribution is used for inference (See Equation 3).

$$p(\mathbf{y} | \mathbf{x}, \mathbf{X}, \mathbf{Y}) = \int p(\mathbf{y} | \mathbf{x}, \mathbf{X}, \mathbf{Y}, \mathbf{w})p(\mathbf{w} | \mathbf{X}, \mathbf{Y})d\mathbf{w} \quad (3)$$

where $\mathbf{w} = \{\mathbf{W}^{(i)}\}_{i=1}^L$. Equation 3 is intractable. When a regular neural network has dropouts, it's possible to approximate the posterior predictive distribution by performing T stochastic forward passes and averaging the results. This is called "*Monte-Carlo dropout*" [6]. In practice, the difference between the Monte-Carlo model averaging and weight scaling is minimal. However, we can use the variance or entropy of the results of T stochastic forward passes to estimate the model uncertainty.

2.2 Batch normalization

Batch normalization was first introduced to address the *internal covariate shift* problem [7]. Normalization is done simply by subtracting the batch mean from every element in the batch and dividing it by the batch standard deviation. It's empirically shown that batch normalization allows higher learning rates to be used, and thus leading to faster convergence.

2.3 Whitening inputs of neural networks

Whitening decorrelates and normalizes inputs. Instead of using computationally expensive existing techniques, such as ICA (independent component analysis) [8], it was shown that using a batch normalization layer followed by a dropout layer can also achieve whitening [9]. The authors called this the IC (Independent-Component) layer. They argued that their IC layer can reduce the mutual information and correlation between the neurons by a factor of p^2 and p , respectively, where p is the dropout probability.

The authors suggested that an IC layer should be placed before a weight layer. They empirically showed that modifying ResNet [10] to include IC layers led to a more stable training process, faster convergence, and better convergence limit.

2.4 Skip connections

Skip connections were first introduced in convolutional neural networks (CNNs) [10]. Before then, having deeper CNNs with more layers didn't necessarily lead to better performance, but rather they suffered from the degradation problem. ResNets solved this problem by introducing skip connections. They managed to train deep CNNs, even with 152 layers, which wasn't seen before, and showed great results on some computer vision benchmark datasets.

3 Methodology

3.1 Motivation

We want to take advantage of the previous works on whitening neural network inputs [9] and skip connections [10], and apply them to MLPs. In each of their original papers, the ideas were tested on CNNs, not on MLPs. However, considering that both a fully connected layer and a convolutional layer are a linear function of f that satisfies Equation 4, and that their main job is feature extraction, we assume that MLPs can also benefit from them.

$$f(\mathbf{x} + \mathbf{y}) = f(\mathbf{x}) + f(\mathbf{y}) \quad \text{and} \quad f(a\mathbf{x}) = af(\mathbf{x}) \quad (4)$$

The biggest difference between a convolutional layer and a fully connected layer is that the former works locally, especially spatially, but the latter works globally.

Also, even the latest neural network architectures, such as the Transformer [11], don't use IC layers and skip connections within their fully connected layers. They can potentially benefit from our work.

3.2 Neural network architecture

Our MLP closely follows [9] and [10]. Our MLP is composed of a series of two basic building blocks. One is called the residual block and the other is called the downsample block.

The residual block starts with an IC layer, followed by a fully connected layer and ReLU nonlinearity. This is repeated twice, as it was done in the original ResNet paper [10]. The skip connection is added before the last ReLU layer (See Equation 5).

$$\mathbf{y} = \text{ReLU}(\mathbf{W}^{(2)} \text{Dropout}(\text{BN}(\text{ReLU}(\mathbf{W}^{(1)} \text{Dropout}(\text{BN}(\mathbf{x})))))) + \mathbf{x} \quad (5)$$

where \mathbf{x} is an input vector to the residual block, BN is a batch normalization layer, Dropout is a dropout layer, ReLU is a ReLU nonlinearity, \mathbf{W}_1 is the first fully connected layer, and \mathbf{W}_2 is the second fully connected layer. This building preserves the dimension of the input vector. That is, $\mathbf{x}, \mathbf{y} \in \mathbb{R}^N$ and $\mathbf{W}^{(1)}, \mathbf{W}^{(2)} \in \mathbb{R}^{N \times N}$. This is done intentionally so that the skip connections can be made easily.

The downsample block also starts with an IC layer, followed by a fully connected layer and ReLU nonlinearity (See Equation 6).

$$\mathbf{y} = \text{ReLU}(\mathbf{W} \text{Dropout}(\text{BN}(\mathbf{x}))) \quad (6)$$

The dimension is halved after the weight matrix \mathbf{W} . That is, $\mathbf{x} \in \mathbb{R}^N$, $\mathbf{W} \in \mathbb{R}^{\frac{N}{2} \times N}$, and $\mathbf{y} \in \mathbb{R}^{\frac{N}{2}}$. This block reduces the number of features so that the network can condense information which will later be used for classification or regression.

After a series of the two building blocks, one fully connected layer is appended at the end for the regression or classification task. We will only carry out classification tasks in our experiments for

simplicity. Therefore, the softmax function is used for the last nonlinearity and the cross-entropy loss will be used for the loss function in Equation 2.

Although our MLP consists of the functions and layers that already exist, we haven't yet found any works that look exactly like ours. The most similar works were found at [12] and [13].

[12] used an MLP, whose order is $FC \rightarrow BN \rightarrow ReLU \rightarrow Dropout \rightarrow FC \rightarrow BN \rightarrow ReLU \rightarrow Dropout$, where FC stands for fully-connected. A skip connection is added after the last $Dropout$. Since $ReLU$ is added between BN and $Dropout$, their MLP architecture does not benefit from whitening.

[13] used an MLP, whose order is $FC \rightarrow BN \rightarrow Dropout \rightarrow FC \rightarrow BN \rightarrow Dropout \rightarrow ReLU$, where FC stands for fully-connected. A skip connection is added before the last $ReLU$. Their block does include $BN \rightarrow Dropout \rightarrow FC$, like our MLP. However, there is no nonlinearity after the FC . Without nonlinearity after a fully-connected layer, it won't benefit from potentially more complex decision boundaries.

Since our neural network architecture includes dropouts, we will take advantage of the Monte-Carlo dropout [6] to model the prediction uncertainty that a model makes on test examples.

4 Experiments

4.1 Age and gender datasets

To test our method in Section 3.2, we chose the age and gender datasets [14] [15]. The Adience dataset [14] is a five-fold cross-validation dataset. This dataset comes from Flickr album photos and is the most commonly used dataset for age and gender estimation. You can check the leaderboard at <https://paperswithcode.com/>. The IMDB-WIKI dataset [15] is bigger than Adience. It comes from celebrity images from IMDB and Wikipedia. We'll report the performance metrics (i.e. the cross entropy loss and accuracy) on the Adience dataset with five-fold cross-validation so that we can compare our results with others. The IMDB-WIKI dataset is only used for hyperparameter tuning and pretraining.

The original images from the Adience dataset have the size of $816 \times 816 \times 3$ pixels. Although CNNs are known to be good at extracting spatial features from such data, the point of our experiment is to test and compare the MLP architectures. Therefore, we transform the images to fixed-size vectors.

We use RetinaFace [16] to get the bounding box and the five facial landmarks, with which we can affine-transform the images to arrays of size $112 \times 112 \times 3$ pixels (See Figure 1). Besides reducing the size of the data, this also has a benefit of removing background noise.



(a) Original image, $816 \times 816 \times 3$ pixels



(b) Affine-transformed to $112 \times 112 \times 3$ pixels

Figure 1: A sample image from the Adience dataset. Instead of using the original images, such as Figure 1a, we use affine-transformed images, as in Figure 1b.

Next we use ArcFace [17] to further reduce the size and extract features from the affine-transformed images. ArcFace is a powerful face-embedding extractor which can be used for face recognition. This transformation transforms $112 \times 112 \times 3$ pixel arrays to 512-dimensional vectors. It was shown in [18] that a classifier can be built on such vectors to classify gender. We take this approach further to even classify age as well.

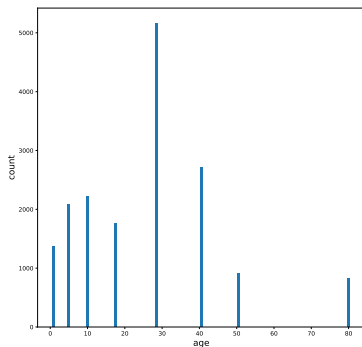
Table 1 shows the number of data samples before and after removal, along with the gender distribution. Table 2 shows the number of data samples removed and the reason why they were removed. Figure 2 shows the age distribution of each dataset. The IMDB-WIKI dataset has a more fine-grained age distribution than the Adience dataset.

Dataset	number of images before removal	number of images after removal	Gender	
			female	male
Adience	19,370	17,055 (88.04% of original)	9,103	7,952
IMDB-WIKI	523,051	398,251 (76.14% of original)	163,228	235,023

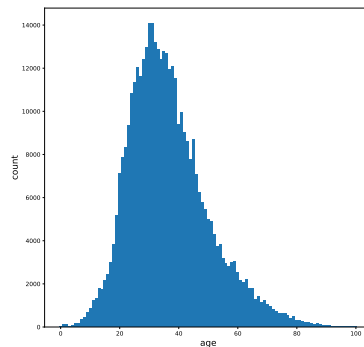
Table 1: The statistics of the Adience and IMDB-WIKI datasets

Dataset	failed to process image	no age found	no gender found	no face detected	bad face quality (det_score <0.9)	more than one face	no face embeddings	total
Adience	0	748	1,170	322	75	0	0	2,315 (11.95% of original)
IMDB-WIKI	33,109	2,471	10,938	24,515	4,283	49,457	27	124,800 (23.86 % of original)

Table 2: The number of images removed



(a) The age distribution of the Adience dataset



(b) The age distribution of the IMDB-WIKI dataset

Figure 2: The age distribution of the Adience (Figure 2a) and IMDB-WIKI (Figure 2b) datasets. Adience has coarse-grained 8 age categories (i.e. 0-2, 4-6, 8-12, 15-20, 25-32, 38-43, 48-53, and 60-100), while IMDB-WIKI has fine-grained 101 age categories (i.e. from 0 to 100).

4.2 Training and hyperparameters

We first pretrain three MLPs with the IMDB-WIKI dataset:

1. 2-class gender classification.
2. 8-class age classification¹.
3. 101-class age classification.

There are a number of hyperparameters to be considered to train the models. Some of them are just fixed by following the best practices. For example, we fix the dropout rate to 0.05 as it was shown in [9]. We use AdamW [19] for the optimizer, as it was proven to be better than using vanilla Adam [20]. And we use ExponentialLR for learning rate scheduling. Now the remaining hyperparameters to be determined are the number of residual blocks, number of downsample blocks, batch size, initial learning rate, weight decay coefficient, and multiplicative factor of learning rate decay. They were determined using automatic hyperparameter tuning with Ray Tune [21]. We also use automatic mixed precision to speed up training. 10% of the IMDB-WIKI dataset was held-out from the other

¹The 101 age categories are converted to the 8 categories by projecting them to the nearest numbers of the Adience dataset.

model	training loss mean (std.)	training accuracy mean (std.)	validation loss mean (std.)	validation accuracy mean (std.)	test loss mean (std.)	test accuracy mean (std.)
2-class gender classification, random init	0.0650 (0.0074)	0.9800 (0.0030)	0.1180 (0.0150)	0.9639 (0.0063)	0.4353 (0.0785)	0.8406 (0.0273)
2-class gender classification, random init, no dropout	0.0459 (0.0050)	0.9874 (0.0020)	0.1044 (0.0109)	0.9672 (0.0039)	0.4047 (0.0810)	0.8413 (0.0326)
2-class gender classification, random init, no IC	0.1879 (0.0618)	0.9425 (0.0102)	0.2067 (0.0623)	0.9336 (0.0121)	0.4622 (0.0914)	0.8207 (0.0389)
2-class gender classification, random init, no skip connections	0.0666 (0.0067)	0.9805 (0.0021)	0.1176 (0.0130)	0.9614 (0.0052)	0.4217 (0.0865)	0.8340 (0.0345)
2-class gender classification, random init, no IC, no skip connections	0.6141 (0.1254)	0.6119 (0.1568)	0.6144 (0.1242)	0.6151 (0.1557)	0.6581 (0.0581)	0.5847 (0.1015)
2-class gender classification, pretrained	0.0332 (0.0021)	0.9917 (0.0009)	0.0810 (0.0167)	0.9772 (0.0049)	0.3120 (0.0604)	0.8887 (0.0255)
2-class gender classification, pretrained, no dropout	0.0400 (0.0027)	0.9899 (0.0013)	0.0841 (0.0192)	0.9753 (0.0042)	0.2768 (0.0457)	0.8986 (0.0198)
2-class gender classification, pretrained, no IC	0.0438 (0.0037)	0.9880 (0.0011)	0.0895 (0.0149)	0.9743 (0.0047)	0.2679 (0.0676)	0.9066 (0.0248)
2-class gender classification, pretrained, no skip connections	0.1110 (0.0050)	0.9707 (0.0021)	0.1389 (0.0128)	0.9596 (0.0059)	0.2833 (0.0338)	0.8937 (0.0171)
2-class gender classification, pretrained, no IC, no skip connections	0.0633 (0.0033)	0.9833 (0.0012)	0.1041 (0.0177)	0.9693 (0.0061)	0.2835 (0.0659)	0.9034 (0.0227)
2-class gender classification SOTA [22]						<i>0.8966</i>
8-class age classification, random init	0.0147 (0.0075)	0.9974 (0.0017)	0.2299 (0.0273)	0.9342 (0.0064)	1.6409 (0.1889)	0.5482 (0.0391)
8-class age classification, random init, no dropout	0.0139 (0.0079)	0.9976 (0.0019)	0.2259 (0.0303)	0.9343 (0.0086)	1.6301 (0.1815)	0.5437 (0.0413)
8-class age classification, random init, no IC	0.2188 (0.0329)	0.9288 (0.0138)	0.4496 (0.0480)	0.8596 (0.0126)	1.5591 (0.1445)	0.5332 (0.0403)
8-class age classification, random init, no skip connections	0.0157 (0.0039)	0.9971 (0.0008)	0.2330 (0.0261)	0.9331 (0.0079)	1.6680 (0.1392)	0.5395 (0.0374)
8-class age classification, random init, no IC, no skip connections	0.4202 (0.0797)	0.8359 (0.0428)	0.7315 (0.0969)	0.7548 (0.0431)	2.0719 (0.2454)	0.4068 (0.0529)
8-class age classification, pretrained	0.0442 (0.0111)	0.9906 (0.0027)	0.2498 (0.0274)	0.9237 (0.0076)	1.3567 (0.1020)	0.6086 (0.0283)
8-class age classification, pretrained, no dropout	0.0454 (0.0145)	0.9906 (0.0036)	0.2721 (0.0262)	0.9156 (0.0081)	1.3589 (0.0774)	0.5968 (0.0187)
8-class age classification, pretrained, no IC	0.0904 (0.0202)	0.9799 (0.0057)	0.3133 (0.0210)	0.9013 (0.0082)	1.3406 (0.0900)	0.6032 (0.0308)
8-class age classification, pretrained, no skip connections	0.0538 (0.0181)	0.9873 (0.0048)	0.2599 (0.0226)	0.9210 (0.0083)	1.3822 (0.0963)	0.6047 (0.0270)
8-class age classification, pretrained, no IC, no skip connections	0.1052 (0.0128)	0.9751 (0.0037)	0.3307 (0.0252)	0.8932 (0.0087)	1.3568 (0.1311)	0.5937 (0.0357)
modified 8-class age classification, random init	0.0188 (0.0040)	0.9968 (0.0008)	0.2354 (0.0271)	0.9343 (0.0073)	1.6534 (0.1735)	0.5445 (0.0397)
modified 8-class age classification, random init, no dropout	0.0170 (0.0047)	0.9973 (0.0009)	0.2345 (0.0273)	0.9326 (0.0073)	1.6319 (0.1586)	0.5477 (0.0354)
modified 8-class age classification, random init, no IC	0.4539 (0.0472)	0.8340 (0.0192)	0.5811 (0.0408)	0.7933 (0.0183)	1.3348 (0.1425)	0.5329 (0.0372)
modified 8-class age classification, random init, no skip connections	0.0198 (0.0049)	0.9965 (0.0009)	0.2336 (0.0270)	0.9326 (0.0081)	1.6528 (0.1671)	0.5435 (0.0371)
modified 8-class age classification, random init, no IC, no skip connections	0.8561 (0.1304)	0.6270 (0.0584)	0.9393 (0.1106)	0.5967 (0.0519)	1.4231 (0.1128)	0.4270 (0.0388)
modified 8-class age classification, pretrained	0.0455 (0.0116)	0.9913 (0.0027)	0.2623 (0.0272)	0.9195 (0.0080)	1.3636 (0.0694)	0.6005 (0.0233)
modified 8-class age classification, pretrained, no dropout	0.0444 (0.0127)	0.9918 (0.0028)	0.2679 (0.0277)	0.9196 (0.0078)	1.4226 (0.1403)	0.5916 (0.0362)
modified 8-class age classification, pretrained, no IC	0.1100 (0.0216)	0.9726 (0.0064)	0.3482 (0.0238)	0.8930 (0.0065)	1.3880 (0.0790)	0.6030 (0.0216)
modified 8-class age classification, pretrained, no skip connections	0.0450 (0.0078)	0.9908 (0.0021)	0.2650 (0.0285)	0.9188 (0.0080)	1.4405 (0.0882)	0.5985 (0.0226)
modified 8-class age classification, pretrained, no IC, no skip connections	0.1311 (0.0221)	0.9655 (0.0068)	0.3538 (0.0230)	0.8890 (0.0065)	1.3887 (0.1497)	0.5967 (0.0344)
8-class age gender classification SOTA [23]						<i>0.6747</i>

Table 3: The loss and accuracy of the trained models. The “modified” 8-class age classification models are the ones that were initially trained for the 101-class age classification task, but then repurposed to 8-class classification. Random initialization is done with Kaiming He uniform random initialization [24]. We ran five-fold cross validation five times. The reported numbers are the averages of the 25 runs. Early stopping was done to save training time. That’s why some trainings lasted longer epochs than the others.

model is very light-weight, running 512 passes on a CPU was not a problem. See Figure 5 for the faces with low and high entropy. Interestingly, four out of the ten highest entropy faces are either baby or kid faces, which has low frequency in the Adience dataset.

5 Conclusion

MLPs have a long history in neural networks. Although they are ubiquitously used, a systematic research to generalize them has been missing. By placing an IC (Independent-Component) layer to whiten inputs before every fully-connected layer, followed by ReLU nonlinearity, and adding skip connections, our MLP empirically showed it can have a better convergence limit, when its weights are initialized from a pretrained network. Also, since our MLP architecture includes dropouts, we were able to show that our MLP can estimate the uncertainty of model predictions. In the future work, we want to test our idea on different datasets to see how well it can generalize.

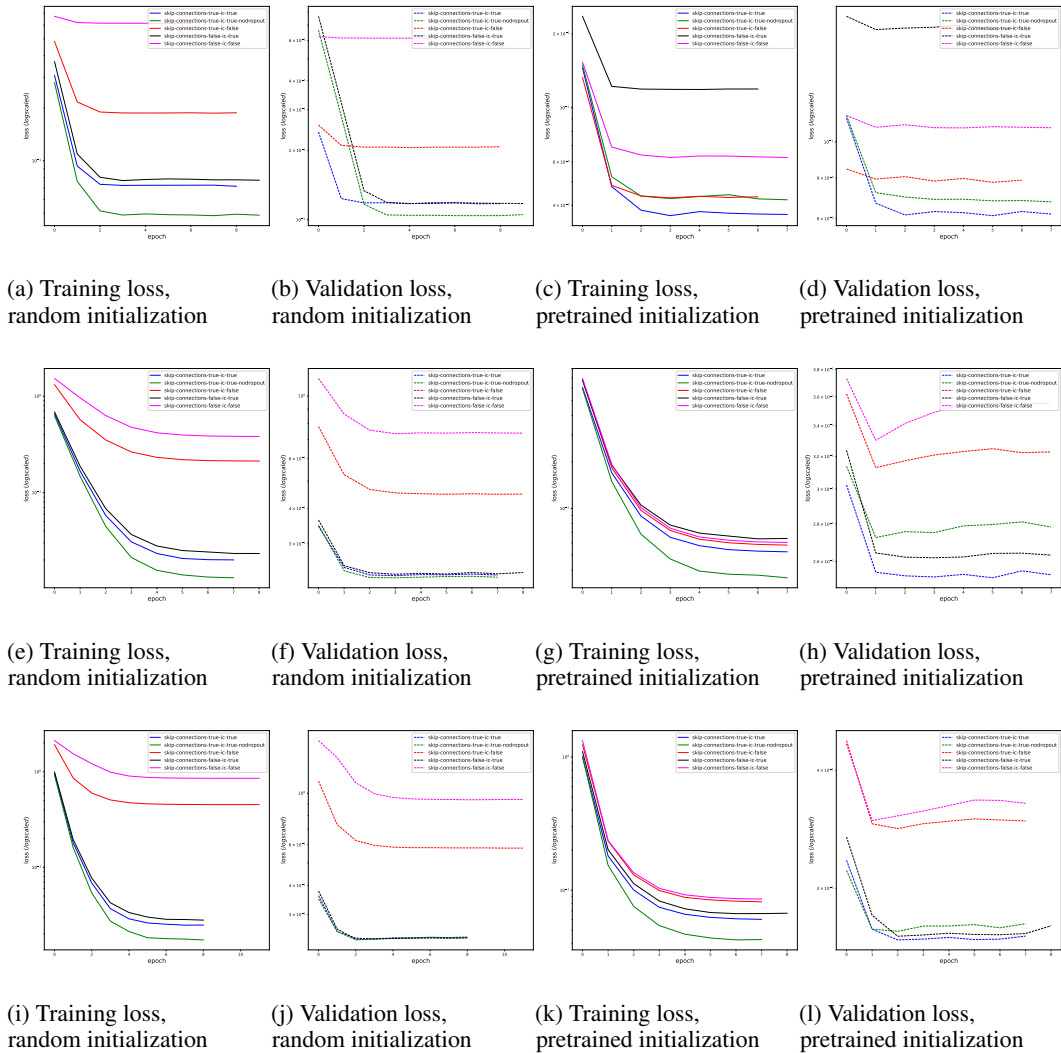


Figure 4: Cross-entropy loss vs. epoch in training gender and classification, with random and pretrained initialization. The top, middle, and the bottom rows are the 2-class gender, 8-class age, and “modified” 8-class age classification task, respectively. Random initialization is done with Kaiming He uniform random initialization [24]. We ran five-fold cross validation five times. The reported numbers are the averages of the 25 runs.

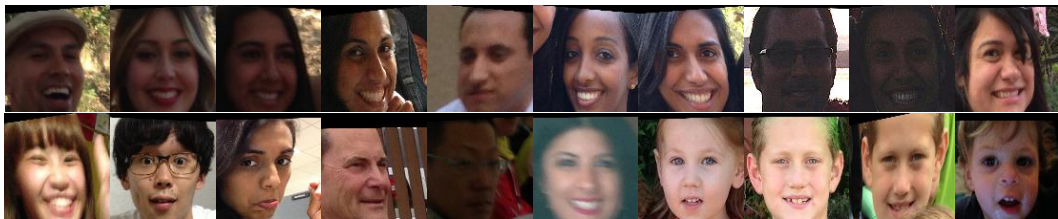


Figure 5: Top row faces are the ten Adience pictures with the lowest entropy. Their entropy values are all zero, which means that the model is 100% sure of its predictions. Bottom row faces are the ten Adience ones with the highest entropy. Their entropy values are all close to 0.6931, which is the maximum entropy for a binary classification.

References

- [1] F. Rosenblatt. The perceptron: a probabilistic model for information storage and organization in the brain. *Psychological review*, 65 6:386–408, 1958.
- [2] Vinod Nair and Geoffrey E. Hinton. Rectified linear units improve restricted boltzmann machines. In *Proceedings of the 27th International Conference on International Conference on Machine Learning*, ICML'10, page 807–814, Madison, WI, USA, 2010. Omnipress.
- [3] D. Rumelhart, Geoffrey E. Hinton, and Ronald J. Williams. Learning representations by back-propagating errors. *Nature*, 323:533–536, 1986.
- [4] Nitish Srivastava, Geoffrey Hinton, Alex Krizhevsky, Ilya Sutskever, and Ruslan Salakhutdinov. Dropout: A simple way to prevent neural networks from overfitting. *Journal of Machine Learning Research*, 15(56):1929–1958, 2014.
- [5] Naftali Tishby, Esther Levin, and Sara A. Solla. Consistent inference of probabilities in layered networks: Predictions and generalization. In Anon, editor, *IJCNN Int Jt Conf Neural Network*, pages 403–409. Publ by IEEE, December 1989. IJCNN International Joint Conference on Neural Networks ; Conference date: 18-06-1989 Through 22-06-1989.
- [6] Yarın Gal and Zoubin Ghahramani. Dropout as a bayesian approximation: Representing model uncertainty in deep learning. In Maria Florina Balcan and Kilian Q. Weinberger, editors, *Proceedings of The 33rd International Conference on Machine Learning*, volume 48 of *Proceedings of Machine Learning Research*, pages 1050–1059, New York, New York, USA, 20–22 Jun 2016. PMLR.
- [7] Sergey Ioffe and Christian Szegedy. Batch normalization: Accelerating deep network training by reducing internal covariate shift. In *Proceedings of the 32nd International Conference on International Conference on Machine Learning - Volume 37*, ICML'15, page 448–456. JMLR.org, 2015.
- [8] A. Hyvärinen and E. Oja. Independent component analysis: algorithms and applications. *Neural Networks*, 13(4):411–430, 2000.
- [9] Guangyong Chen, Pengfei Chen, Yujun Shi, Chang-Yu Hsieh, Benben Liao, and Shengyu Zhang. Rethinking the usage of batch normalization and dropout in the training of deep neural networks, 2019.
- [10] Kaiming He, Xiangyu Zhang, Shaoqing Ren, and Jian Sun. Deep residual learning for image recognition. In *2016 IEEE Conference on Computer Vision and Pattern Recognition (CVPR)*, pages 770–778, 2016.
- [11] Ashish Vaswani, Noam Shazeer, Niki Parmar, Jakob Uszkoreit, Llion Jones, Aidan N. Gomez, undefinedukasz Kaiser, and Illia Polosukhin. Attention is all you need. In *Proceedings of the 31st International Conference on Neural Information Processing Systems, NIPS'17*, page 6000–6010, Red Hook, NY, USA, 2017. Curran Associates Inc.
- [12] Julieta Martinez, Rayat Hossain, J. Romero, and J. Little. A simple yet effective baseline for 3d human pose estimation. *2017 IEEE International Conference on Computer Vision (ICCV)*, pages 2659–2668, 2017.
- [13] Ana C Q Siravenha, Mylena N F Reis, Iraquitan Cordeiro, Renan Arthur Tourinho, Bruno D. Gomes, and Schubert R. Carvalho. Residual mlp network for mental fatigue classification in mining workers from brain data. In *2019 8th Brazilian Conference on Intelligent Systems (BRACIS)*, pages 407–412, 2019.
- [14] Eran Eiding, Roe Enbar, and Tal Hassner. Age and gender estimation of unfiltered faces. *IEEE Transactions on Information Forensics and Security*, 9(12):2170–2179, 2014.
- [15] Rasmus Rothe, Radu Timofte, and Luc Van Gool. Dex: Deep expectation of apparent age from a single image. In *IEEE International Conference on Computer Vision Workshops (ICCVW)*, December 2015.
- [16] Jiankang Deng, Jia Guo, Evangelos Ververas, Irene Kotsia, and Stefanos Zafeiriou. Retinaface: Single-shot multi-level face localisation in the wild. In *Proceedings of the IEEE/CVF Conference on Computer Vision and Pattern Recognition (CVPR)*, June 2020.
- [17] Jiankang Deng, Jia Guo, Niannan Xue, and Stefanos Zafeiriou. Arcface: Additive angular margin loss for deep face recognition. In *2019 IEEE/CVF Conference on Computer Vision and Pattern Recognition (CVPR)*, pages 4685–4694, 2019.

- [18] Avinash Swaminathan, Mridul Chaba, Deepak Kumar Sharma, and Yogesh Chaba. Gender classification using facial embeddings: A novel approach. *Procedia Computer Science*, 167:2634–2642, 2020. International Conference on Computational Intelligence and Data Science.
- [19] I. Loshchilov and F. Hutter. Decoupled weight decay regularization. In *ICLR*, 2019.
- [20] Diederik P. Kingma and Jimmy Ba. Adam: A method for stochastic optimization. *CoRR*, abs/1412.6980, 2015.
- [21] Richard Liaw, Eric Liang, Robert Nishihara, Philipp Moritz, Joseph E Gonzalez, and Ion Stoica. Tune: A research platform for distributed model selection and training. *arXiv preprint arXiv:1807.05118*, 2018.
- [22] Steven C. Y. Hung, Cheng-Hao Tu, Cheng-En Wu, Chien-Hung Chen, Yi-Ming Chan, and Chu-Song Chen. Compacting, picking and growing for unforgetting continual learning. *CoRR*, abs/1910.06562, 2019.
- [23] Ke Zhang, Na Liu, Xingfang Yuan, Xinyao Guo, Ce Gao, Zhenbing Zhao, and Zhanyu Ma. Fine-grained age estimation in the wild with attention lstm networks. *IEEE Trans. Cir. and Sys. for Video Technol.*, 30(9):3140–3152, September 2020.
- [24] Kaiming He, X. Zhang, Shaoqing Ren, and Jian Sun. Delving deep into rectifiers: Surpassing human-level performance on imagenet classification. *2015 IEEE International Conference on Computer Vision (ICCV)*, pages 1026–1034, 2015.